Creating 3D constructs with cranial neural crest-derived cell lines using a bio-3D printer

Authors:

Masahide Taguchi[a], Shohei Yoshimoto[b,c], Kanako Suyama[a], Satoko Sumi[a], Shirabe Ohki[a], Kayoko Ogata[d], Ryota Fujimoto[e], Daiki Murata[e], Koichi Nakayama[e], Kyoko Oka[a,c]

[a] Section of Pediatric Dentistry, Department of Oral Growth and Development, Fukuoka Dental College, Fukuoka, Japan

[b] Section of Pathology, Department of Morphological Biology, Fukuoka Dental College, Fukuoka, Japan

[c] Oral Medicine Research Center, Fukuoka Dental College, Fukuoka, Japan

[d] Department of Legal Medicine, Graduate School of Medical Sciences, Kanazawa University

[e] Center for Regenerative Medicine Research, Faculty of Medicine, Saga University, Saga, Japan

Authors:

Masahide Taguchi, E-mail: mtaguchi@fdcnet.ac.jp

Shohei Yoshimoto, E-mail: yoshimoto@fdcnet.ac.jp

Kanako Suyama, E-mail: chikushi@fdcnet.ac.jp

Satoko Sumi, E-mail: sumi@fdcnet.ac.jp

Shirabe Ohki, E-mail: meeenl0dy@gmail.com

Kayoko Ogata, E-mail: ogata@med.kanazawa-u.ac.jp

Ryota Fujimoto, E-mail: r-fujimoto@nakayama-labs.com

Daiki Murata, E-mail: daiki_net_official@yahoo.co.jp

Koichi Nakayama, E-mail: nakayama@nakayama-labs.com

Kyoko Oka, E-mail: okak@fdcnet.ac.jp

Corresponding author:

Kyoko Oka

Section of Pediatric Dentistry, Department of Oral Growth and Development,

Fukuoka Dental College, Fukuoka, Japan

2-15-1 Tamura, Sawara-ku, Fukuoka 814-0193, Japan

E-mail: okak@fdcnet.ac.jp

ORCID: 0000-0002-1648-1596

TEL: +81-92-801-0411

FAX: +81-92-801-0692

ABSTRACT

Objectives: The development of bio-three-dimensional (bio-3D) printers has led to significant advances in regenerative medicine. Three-dimensional constructs, including spheroids, are maintained by extracellular matrix proteins secreted by cells so that the cells can be cultured in conditions closer to the physiological environment. This study aimed to create a useful 3D construct as a model of the dentin-pulp complex. **Methods:** We examined the expression patterns of extracellular matrix proteins and cell proliferation areas in a 3D construct created using O9-1 cells derived from cranial neural crest cells of mice. The 3D construct was created by sticking the spheroid cultures onto a needle array using a bio-3D printer. **Results:** Cell proliferation areas along with characteristic expression of tenascin C and DMP1 were evaluated. The expression of tenascin C and DMP1 was significantly enhanced in the spheroids compared to that in two-dimensional cultures. Moreover, cell proliferation regions and tenascin C expression were confirmed in the outer layer of spheroids in the embryonic stem cell medium, with insignificant DMP1 expression being observed. Interestingly, in a 3D construct cultured in calcification-induction medium, DMP1 expression was promoted, and DMP1-positive cells existed in

the outermost layer without overlapping with tenascin C expression.

Conclusions: The extracellular matrix proteins, tenascin C and DMP1, were expressed in a polarized manner in spheroids and 3D constructs, similar to the findings in the dental papilla. Therefore, these 3D constructs show potential as artificial models for studying odontogenesis.

Keywords: 3D constructs; spheroid; bio-3D printer; tenascin C

1 INTRODUCTION

The technique of three-dimensional (3D) cell culturing has been developed and popularized in the field of tissue engineering. Spheroid formation with cells is one method for creating 3D engineered constructs, produced by spontaneous cell aggregation during culture in non-coated plates [1]. One advantage of spheroid cultures compared to classical two-dimensional (2D) systems is that we can study and examine cell behaviors under conditions closer to the physiological state [2]. Spheroid cultures might provide an ideal microenvironment through optimal cell proliferation, differentiation, and cell-to-cell interactions, because each cell can exist in the spheroid with polarization.

To create an appropriately sized artificial organ outside the body for application in clinical practice, spheroids must be piled and stacked to create a single large 3D construct. Recently, various types of bioprinters have been developed, including inkjet, extruder, and laser-assisted types. One interesting method involves creating 3D constructs by sticking spheroids onto extremely fine microneedles (modeled after the kenzan used in the Japanese art of ikebana [flower arrangement]) [3]. This method has performed well. For example, blood vessels created with a KENZAN-type bio-3D printer are now

being applied in humans [4]. One advantage of the KENZAN-type bio-3D printer is that the construct is formed by extracellular matrix proteins secreted from the spheroid body itself, similar to the process of tissue development in humans. The shape of the construct can also be designed by piling spheroids on the microneedle array. This would enable immature cells to differentiate at a suitable site at a suitable timing by themselves. As an example, mandibular development starts as a regional aggregate of immature mesenchymal cells, which proliferate and differentiate into various cell types, such as osteoblasts, chondrocytes, fibroblasts, tenocytes, and myofibroblasts, according to the programmed sites and timings [5, 6]. This means that both hard and soft tissues have a common origin, which suggests that the extracellular environment, including extracellular matrix proteins, are important in the process of selection of the right cells and right positions by the developing tissues themselves.

Teeth are highly organized organs created by epithelial and mesenchymal interactions among hard tissues [7]. During tooth development, cranial neural crest cell-derived mesenchymal cells aggregate under an inner enamel epithelium called the dental papilla [8, 9]. Odontoblasts are one component of the dental papilla that align in a polarized manner in the outer layer of the dental

papilla adjacent to ameloblasts, and secrete dentin matrix [9, 10]. Odontoblasts retreat to the pulp side during the secretion of dentin matrix, with dentin matrix formation proceeding outside the dental papilla. The extracellular matrix thus clearly plays important roles in these behaviors of the odontoblast. We wondered whether a KENZAN-type bio-3D printer could be used to create constructs of neatly arranged connective and hard tissues, such as the dentin-pulp complex.

We previously focused on extracellular matrix expression during the development of organs in which soft and hard tissues are continuous, such as the hard and soft palate or cementum and periodontal ligament fibrous tissues [11-13]. Among these, we showed the importance of the characteristic expression of tenascin C and periostin in the palatal processes during palatogenesis, particularly in terms of the roles of these proteins in suppressing the differentiation of immature mesenchymal cells into osteogenic cells and maintaining connective tissue constructs [11, 12]. Through these studies examining different patterns of extracellular matrix expression during tissue development in mice, related to the regulated cell differentiation required to form

refined tissues, we became interested in the spontaneous patterning of extracellular matrix expression in vitro using 3D culture systems.

In this study, we tried to create a 3D construct mirroring the dentin-pulp complex using bioprinting techniques, and examined the unique expression patterns of tenascin C brought about by 3D construction.

2 MATERIALS AND METHODS

2.1 Cell culture

O9-1 cells (Merck Millipore, Darmstadt, Germany) were derived from mass cultures of *Wnt1 -Cre/R26R -GFP* reporter-expressing cranial neural crest cells from E8.5 mouse embryos [14]. The O9-1 cells were maintained in embryonic stem (ES) cell medium containing 15% fetal bovine serum and mouse leukemia inhibitory factor (mLIF; Merck Millipore), or endothelial growth medium (EGM)/fibroblast growth medium (FGM) as an even mixture (FGM™-2 BulletKit™; Lonza, Basel, Switzerland and EGM™-2 BulletKit™; Lonza).

2.2 Spheroid formation and measurement

O9-1 cells were cultured in non-adhesion plates with 1.0–5.0 ×10^4 cells/well (PrimeSurface 96U Plate; Sumitomo Bakelite, Tokyo, Japan) in ES cell medium or EGM/FGM. O9-1 spheroids were cultured in a humidified atmosphere with 5% CO_2 at 37°C. The diameter of each spheroid colony was measured 24, 48, and 72 h after harvest (n = 16). Spheroid diameters were measured using B3D designer software (Cyfuse Biomedical K.K., Tokyo, Japan).

2.3 Supplements for induction of calcification

The calcification induction medium included 3.8 mmol/L calcium. This medium was created as a mixture of 0.1 mol/L Ca solution (Nacalai Tesque, Kyoto, Japan) added to high-glucose Dulbecco's modified Eagle's medium (Merck Millipore) supplemented with 20% fetal bovine serum and 1% penicillin/streptomycin.

2.4 Procedure for creating a scaffold-free 3D construct

The 3D construct was fabricated using a bio-3D printer (Regenova; Cyfuse Biomedical K.K.) and needle array (hollow 9 × 9 Kenzan; Cyfuse Biomedical K.K.). Briefly, cells (3.5 ×10^4 cells/well) were inoculated into three 96-well non-

adhesion plates (PrimeSurface 96U Plate; Sumitomo Bakelite, Tokyo, Japan) and cultured in ES cell medium (Figures 1A and B). After incubation for 48 h, the cells formed spheroids with diameters of approximately 550 μm (Figure 1C). These spheroids were then arranged on the KENZAN, meaning that each spheroid was pierced by microneedles using the bio-3D printer and printed according to a pre-made design using Bio 3D designer software (Cyfuse Biomedical K.K.), as previously reported [3]. This process takes approximately 1.5 h. After printing, the 3D construct was incubated in culture medium (Complete ES cell medium or calcification induction medium) with the needle array and perfusion by a roller pump at 2 mL/min for 7 days (Figure 1D). On Day 7 after printing, each spheroid was fused and the 3D construct was removed from the needle array (Figures 1E and F).

2.5 RNA *in situ* hybridization and immunostaining for spheroids and 3D constructs

Spheroids and 3D constructs were fixed with 4% paraformaldehyde in phosphate-buffered saline solution. The paraffin embedding protocol for spheroids has been described previously [15]. Paraffin-embedded tissue blocks

were cut into 5-μm-thick sections for hematoxylin and eosin (HE) staining, immunohistochemical staining, and RNA in situ hybridization (ISH). As primary antibodies, mouse Ki-67 monoclonal antibody (dilution 1:100; Leica Biosystems, Newcastle, UK), rat anti-mouse tenascin C monoclonal antibody (clone 578, dilution 1:100; R&D Systems, Minneapolis, MN, USA), and rabbit anti-mouse periostin (dilution 1:100; OriGene Technologies, Rockville, MD, USA) were applied overnight at 4°C. Secondary antibodies were Histofine biotinylated goat anti-mouse immunoglobulin (Ig)G + rabbit IgG (Nichirei Biosciences, Tokyo, Japan), and goat anti-rat IgG (Abcam, Tokyo, Japan). Nuclei were counterstained with hematoxylin. Specimens treated with biotin-conjugated secondary antibody were sensitized using streptavidin peroxidase (Vector Laboratories, Burlingame, CA, USA) and visualized using a diaminobenzidine kit (Nichirei Biosciences, Tokyo, Japan). Specimens were observed using a fluorescence microscope (BZ-X710; Keyence, Osaka, Japan). To assess the cell proliferation rate of each spheroid, the number of Ki-67-positive cells and nuclei were counted in 100 μm^2 box areas, set in both the outer and inner layers of the spheroid, which were divided concentrically into three sections from the center of the spheroid. The outermost and innermost layers were set as the

outer and inner layers, respectively. Three box areas were randomly selected from each layer in four spheroids each in the ES cell medium and EGM/FGM medium. Expression of dentin sialophosphoprotein (DSPP) and dentin matrix protein 1 (DMP1) mRNA was examined using the RNAscope ISH system (Advanced Cell Diagnostics, Newark, CA, USA) according to the manufacturer's guidelines.

2.6 RNA isolation and real-time quantitative PCR

RNA was extracted from cells using the ReliaPrep™ RNA Miniprep System (Promega, Madison, WI, USA). Synthesis of cDNA was performed using ReverTra Ace® qPCR RT Master Mix (Toyobo, Osaka, Japan). After mixing each cDNA with SsoAdvanced™ Universal SYBR® Green Supermix (Bio-Rad, Hercules, CA, USA), real-time quantitative PCR was performed using LightCycler® 96 System (Roche Diagnostics K.K., Tokyo, Japan). Primer sequences for the genes investigated are shown in Table 1. Results were standardized to the expression of the glyceraldehyde 3-phosphate dehydrogenase gene (*Gapdh*). Each cDNA sample was analyzed in triplicate. The threshold cycle (CT) was defined as the fractional cycle number. Gene

expression values (relative mRNA levels) were expressed as ratios (differences between Ct values: $\Delta Ct = Ct_{interest} - Ct_{Gapdh}$) between the gene of interest and an internal reference gene (*Gapdh*) that provides a normalization factor for the amount of RNA isolated from a specimen. Using the Δ(ΔCt) method, {$\Delta(\Delta Ct) = \Delta Ct_{mutant} - \Delta Ct_{control}$}, the fold change {$2 - \Delta(\Delta Ct)$} was calculated for each control and mutant sample. All data are shown as the mean ± standard deviation, and fold differences in the expression of each gene were calculated according to the ΔΔCT method with normalization to *Gapdh*.

2.7 Statistical analysis

Data are presented as the mean ± standard deviation. Comparisons between groups were made using the Mann–Whitney U test. Values of $P < 0.05$ were considered significant.

3 RESULTS

3.1 Phenotype of spheroids

We cultured O9-1 cells in non-coating plates to form spheroids and decided the protocol was suitable for the KENZAN method. This required creation of

spheroid bodies with not only size within the range of 550–600 μm, but also optimal hardness. The number of cells to be seeded per well was examined using two different culture media. Spheroids formed within 24 h after seeding, and their diameter decreased during culture. As of Day 2, proper spheroid bodies could be created when more than 3.5 $\times 10^4$ O9-1 cells were seeded in ES cell medium and 4.5 $\times 10^4$ cells in EGM/FGM (Figures 2A and B). Next, we examined the histological appearance with HE staining. The tissue condition was healthy in the spheroid formed with ES cell medium (Figure 2C). Proliferating cells showing Ki-67 positivity were observed much more frequently in the outer layer compared to inside the spheroid body with ES cell medium (Figure 2D). The rate of Ki-67-positive cells was significantly higher in the outer layer than the inner layer (Figure 2G). On the other hand, the rate of proliferating cells between the inner and outer regions was almost the same with EGM/FGM (Figures 2F and H).

3.2 Extracellular matrix expression in 2D and 3D cultures

Based on histological observations, we considered that the spheroid construct induced greater formation of extracellular matrix compared to 2D culture. We

therefore performed real-time PCR analysis to examine expressions of type I collagen, periostin, and tenascin C in spheroid and 2D cultured cells using ES cell medium. Expressions of periostin and tenascin C, but not type I collagen, were clearly increased in the spheroid compared to 2D culture (Figures 3A-C). We therefore observed the histological expression patterns of periostin and tenascin C using immunostaining. Periostin was expressed ubiquitously throughout the entire spheroid body, both in ES cell medium and EGM/FGM (Figures 3D and F). Interestingly, tenascin C showed a characteristic expression in the outer layer of the spheroid cultured with ES cell medium (Figure 3E), although little expression of tenascin C was seen in the spheroid cultured with EGM/FGM (Figure 3G).

3.3 Odonto/osteoblastic differentiation marker gene expression

Next, we focused on the expression of odonto/osteoblastic differentiation marker genes between spheroid and 2D culture samples with ES cell medium. Expressions of Runx2, Osterix, and ALP were unchanged between 2D and spheroid cultures (Figures 4A-C). However, DSPP and DMP1 were clearly increased in spheroids compared to 2D cultures (Figures 4D and E). Based on

the elevated expression of DSPP and DMP1 mRNA in the spheroids, we examined their expression patterns using in situ hybridization, and found that DMP1 was also clearly expressed in the outer layer of the spheroids (Figures 4J and O). Using real-time PCR, the relative expression level of DSPP mRNA in spheroids was clearly higher compared to that in the 2D culture (Figure 4D). However, DSPP mRNA expression was not detected in spheroids by in situ hybridization. We concluded that the absolute expression level of DSPP is quite low in spheroids, because the Ct value of DSPP was quite high in real-time PCR (Figures 4I and N). Tenascin C expression was seen in the outer layer of the spheroid with ES cell medium, and Ki-67-positive cells were also observed (Figures 1, 2). Therefore, using DSPP and DMP1 analysis, an adjacent section was used to confirm the expressions of Ki-67 and tenascin C, to test for reproducibility of the observations (Figures 4G, H, K, and L). Evaluation showed that the layer of tenascin C expression was wider and overlapped with the Ki-67-positive cell proliferation area. Additionally, the DMP1 expression area was in the outermost layer of the spheroid and did not overlap with tenascin C expression (Figures 4K-M).

3.4 Trial of 3D construct engineering using the KENZAN method

Based on previous experiments, we decided to use spheroids prepared in ES cell medium as the material for fabricating 3D constructs using the bio-3D printer (KENZAN method). The spheroids to be stuck onto microneedles (KENZAN) were programmed to be cylindrical (Figures 5A and B). Culture of the 3D construct continued with insertion of the microneedle (Figures 5B and C). Three days after printing (Day 8), each spheroid was connected to a microneedle (Figure 5D). By 7 days after the start of printing (Day 12), each spheroid was completely connected. Thereafter, the 3D constructs could be removed from the microneedles as a single mass (Figure 5E).

3.5 Histological analysis of 3D constructs constructed using the bioprinter

The histological appearance with HE-staining of the 3D construct cultured in ES cell medium was examined. The boundaries of each spheroid body could not be identified in the 3D construct (Figures 6A-E). The construct was divided based on cell density and inner, middle, and outer layers in the 3D construct. Cell density was higher in the inner and outer layers of the 3D construct. Ki-67-positive cells were observed in the outer layer (Figure 6G), although the

positivity was not as high as that seen in spheroids. Tenascin C expression was observed at the boundary of the middle and outer layers (Figure 6H), and did not merge with the Ki-67-positive layer (Figures 6G and H). Only little DSPP and DMP1 expression was observed (Figures 6I and J).

3.6 DMP1 expression in 3D constructs cultured with calcification induction medium

We succeeded in constructing 3D constructs using the bio-3D printing KENZAN method, although expression of the odonto/osteoblastic marker, DMP1, was not detected in the construct cultured with ES cell medium. We therefore tried to create 3D constructs with calcification induction medium. After printing the spheroid, the construct was cultured with calcification induction medium. Following 7 days of culture after printing, histological analyses were performed. The construct was divided into inner, middle, and outer layers, and also divided by cell density (Figure 7A). Regions of high cell density in the inner and outer layers were more clearly evident in the 3D construct cultured with calcification induction medium compared to ES cell medium (Figure 6A). Ki-67-positive cells existed only in areas of high cell density (Figures 7B and G). In

contrast, tenascin C was expressed in the inner layer, which was an area of low cell density (Figures 7C and H). mRNA expression of tenascin C was clearly induced in the 3D construct with calcification induction medium (Figure 7K). Interestingly, DMP1 mRNA expression was also clearly induced and detected in the outermost layer of the 3D construct with calcification medium, as observed in spheroid analysis (Figures 7J and M). Tenascin C expression was observed inside the proliferating area of the outer layer, adjacent, but not overlapping with Ki-67 expression. DMP1 expression was observed in the proliferating, Ki-67-positive layer, but showed no overlap with tenascin C (Figures 7G, H, and J).

4 DISCUSSION

As a first step in this study, we needed to determine the appropriate cell numbers and medium conditions for forming an ideal spheroid for reproducing 3D constructs using a bioprinter. We examined the ideal kind of medium for creating spheroids using O9-1 cells that would be optimal for the KENZAN system, and observed the characteristic expression of the extracellular matrix. Spheroids could form with smaller numbers of O9-1 cells with ES cell medium compared to EGM/FGM. This could be because higher cell proliferation in the

outer layer of the spheroid, at the site where tenascin C is expressed with ES cell medium, leads to a size advantage in terms of growth of the spheroid. It is possible that the growth factors (endothelial growth factor and fibroblast growth factor) in EGM/FGM medium induce cell differentiation more than proliferation or extracellular matrix formation. Since it is not necessary to differentiate the cells in a spheroid before forming 3D constructs, we concluded that ES cell medium is more suitable for forming spheroids when using KENZAN methods.

O9-1 cells are an established line of cranial neural crest cells from the first branchial arch in mice, and have the potential to differentiate into several cell lineages that make up the bone, cartilage, nerves, tendons, and connective tissues of the maxillofacial region, as well as the dentine, pulp, and periodontal ligaments of the tooth [8, 14]. In tooth development, cranial neural crest cells aggregate in mesenchyme under the dental lamina and eventually form a component called the dental papilla, which differentiates into cells that play different roles in the inner (pulp cell) and outer (odontoblast) portions of the aggregation, mainly developing into dental pulp and dentin [9]. Cells constituting the dental papilla thus have the potential to differentiate into dento/osteogenic and non-dento/osteogenic cells.

The establishment of various important functions at the inner and outer layers of a single tissue component, such as dental papilla, requires characteristic expression of extracellular matrix proteins. In this study, we clearly showed characteristic extracellular matrix expression, including tenascin C and DMP1, in the spheroid culture. Furthermore, the expression pattern demonstrated polarity in the outer layer of the spheroid, which showed a higher cell proliferative region. The spheroid technique is interesting in that the 3D construct is maintained by extracellular matrix proteins secreted by the constituent cells themselves, thereby eliminating artificial influences, including scaffolding. This spontaneous expression of extracellular matrix with polarity is likely regulated by the oxygen condition. It has been previously reported that LOX-1-positive cells, i.e. hypoxic cells, are detected in the core zone of spheroids [16].

According to the expression pattern of Ki-67/tenascin C /DMP1 in spheroids, we suggest that tenascin C and DMP1 might be candidate extracellular matrices determining the polarity for forming dental pulp and dentin, which originate from dental papilla. In this study, tenascin C was expressed just inside the cell-proliferative outer layer. Taking the spheroid as the starting environment

of the 3D construct, this unique expression pattern might indicate that tenascin C plays a role in allowing proliferatively active cells to spread outward, growing the spheroid, since the presence of tenascin C has been reported to act as an anti-adhesive for fibroblasts [17].

Tenascins are a family of large oligomeric extracellular matrix glycoproteins comprising four members in vertebrates (-C, -R, -X, and -W) [18, 19]. In the tenascin family, tenascin C is widely expressed in mesenchymal tissue at sites of epithelial–mesenchymal interactions during development and wound healing, and around motile cells, including neural crest cells and migrating neuroblasts and glial precursors [16]. We previously reported that tenascin C expression plays an important role in tissue development and repair through promoting fibroblast cell proliferation and differentiation in wound healing and soft palate development [12, 20]. According to our previous investigation, we opine that tenascin C works to prevent calcification at the border of connective tissue and osteogenic tissue.

An in vivo study has already identified tenascin C in dental pulp, which is more prominently associated with dentinogenesis [21]. Furthermore, enhanced expression of tenascin C has been detected in predentin and in reparative

dentin formation after pulp capping [22-24]. Tenascin C is also considered a supportive matrix protein for cell differentiation into odontoblasts, but does not regulate the calcification of dentin, because its expression is restricted to unmineralized regions [22, 24].

On the other hand, the expressions of not only tenascin C, but also DMP1, an odontoblast marker, were promoted in the outer layer of spheroids. Expressions of tenascin C and DMP1 within the spheroid occurred at adjacent sites, but did not overlap. DMP1 is a non-collagen matrix protein expressed in bone and dentin [25]. In teeth, expression of DMP1 has been reported in pulp cells, odontoblastspredentin, dentin, and cementum. In addition, deletion of Dmp1 leads to defects in tooth formation and calcification [25, 26]. DMP1 thus plays an important role in the calcification process. In this study, cells expressing DMP1 mRNA were located in the outermost layers of spheroids, where proliferative activity is high. This DMP1 expression pattern in 3D cultures has also been previously reported using O9-1 cells and using mouse dental pulp-derived cells and immortalized mouse dental papilla cells [16, 27]. Our results of the non-overlapping expressions of tenascin C, which is not an inducer, and DMP1, which is an inducer of calcification, in addition to the results of previous

studies, suggest that O9-1 spheroids might reproduce a similar environment as the in vivo environment of dental papilla.

In this study, however, ES cell medium could not adequately maintain the polarity of the 3D construct, such as that of DMP1 expression, as seen in the spheroid. Therefore, we switched to using the calcification induction medium. The 3D construct cultured with calcification medium showed a highly proliferative area on the outside of the construct, with activity clearly higher than that of the construct with stem cell medium. We opine that DMP1 expression in the spheroid was regulated by an endogenous factor secreted from O9-1 cells. However, this polarity might not be maintained during the process of forming 3D constructs by KENZAN methods, because each spheroid needs to be re-formed. Reproduction of the polarity of cells expressing DMP1 during creation of the 3D construct would lead to the ES cell medium being insufficient. Further clarification is needed to determine the critical factor in calcification induction medium that is required for reproducing DMP1 expression. The area of overlapping expression of tenascin C and cell proliferative areas with Ki-67 in the 3D construct was minimal when using the calcification induction medium. We considered that tenascin C does not regulate cell proliferation directly, but

facilitates cell proliferation outside as a border region between cell proliferating and non-proliferating areas. This role might work better under calcification-induction conditions.

Overall, in this study, we succeeded in creating 3D constructs using a bio-3D printer with the KENZAN method. Histological analysis of the expression of tenascin C and DMP1 in spheroids and 3D constructs created by the bio-3D printer showed no overlap of these expressions. This pattern was similar to the zoning of cell proliferation, differentiation, matrix secretion, and calcification layer formation in a single tissue, as seen in the development of dental papilla. The 3D constructs of the present study might have potential to provide an artificial model for the study of dentin formation. However, although O9-1 cells are an immortalized mouse cell line, they still have some limitations as an artificial model. The present experiments need to be performed using other types of cells, including human mesenchymal stem cells, dental papilla cells extracted from impacted tooth germ, or stem cells from human exfoliated deciduous teeth (SHED).

5 CONCLUSIONS

In summary, a 3D construct of neural crest cell-derived cells was created using a bio-3D printer. Characteristic expressions of tenascin C and DMP1 were observed in the outer layers of the spheroid and 3D constructs, with no evident overlap, similar to the findings in dental papilla. The use of 3D culture methods might allow reproduction of the same expression patterns as those present in vivo. These 3D constructs show potential as artificial models for the study of odontogenesis.

Ethical Approval

No approval from the ethics committee was required for this study.

Acknowledgements

We thank Prof. Kajioka and Dr. Toyoda for kindly providing us with the culture system. We also thank Forte Science Communications for writing assistance. This study was supported in part by the Grants-in-Aid for Scientific Research C (No. 21K10176 to K.O.) and Research Activity Start-up (No. 20K23068 to S.O.) from the Japan Society for the Promotion of Science (JSPS).

Conflict of interest

Koichi Nakayama is a co-founder and shareholder of Cyfuse Biomedical KK, chief technical officer of Arktus Therapeutics, and an inventor/developer designated on the patent for the bio-3D printer. Patent title: Method for Production of Three-Dimensional Structure of Cells; patent number: JP4517125. Patent title: Cell structure production device; patent number: JP5896104. The other authors declare no competing interests regarding the publication of this article.

REFERENCES

[1] Abdolahinia ED, Golestani S, Seif S, Afra N, Aflatoonian K, Jalalian A, et al. A review of the therapeutic potential of dental stem cells as scaffold-free models for tissue engineering application. Tissue Cell 2024;86:102281.

[2] Hishikawa K, Miura S, Marumo T, Yoshioka H, Mori Y, Takato T, et al. Gene expression profile of human mesenchymal stem cells during osteogenesis in three-dimensional thermoreversible gelation polymer. Biochem Biophys Res Commun 2004;14;317(4):1103–7.

[3] Murata D, Arai K, Nakayama K. Scaffold-free bio-3D printing using spheroids as ‘bio-inks’ for tissue (re-)construction and drug response tests. Adv Healthc Mater 2020; e1901831.

[4] Itoh M, Nakayama K, Noguchi R, Kamohara K, Furukawa K, Uchihashi K, et al. Scaffold-free tubular tissues created by a bio-3D printer undergo remodeling and endothelialization when implanted in rat aortae. PLoS One 2015;1;10(9):e0136681.

[5] Oka K, Oka S, Sasaki T, Ito Y, Bringas P Jr, Nonaka K, et al. The role of TGF-beta signaling in regulating chondrogenesis and osteogenesis during mandibular development. Dev Biol 2007;303(1):391–404.

[6] Oka K, Oka S, Hosokawa R, Bringas P Jr, Brockhoff II HS, Nonaka K, et al. TGF-beta mediated Dlx5 signaling plays a crucial role in osteo-chondroprogenitor cell lineage determination during mandible development. Dev Biol 2008;321(2):303–9.

[7] Yu T, Klein OD. Molecular and cellular mechanisms of tooth development, homeostasis and repair. Development 2020;147(2):dev184754.

[8] Chai Y, Jiang X, Ito Y, Bringas JP, Han J, Rowitch DH, et al. Fate of the mammalian cranial neural crest during tooth and mandibular morphogenesis. Development 2000;127(8):1671–9.

[9] Jing J, Feng J, Yuan Y, Guo T, Lei J, Pei F, et al. Spatiotemporal single-cell regulatory atlas reveals neural crest lineage diversification and cellular function during tooth morphogenesis. Nat Commun 2022;13(1):4803.

[10] Lee M, Lee YS, Shon W-J, Park J-C. Physiologic dentin regeneration: its past, present, and future perspectives. Front Physiol 2023;14:1313927.

[11] Oka K, Honda JM, Tsuruga E, Hatakeyama Y, Isokawa K, Sawa Y. Roles of collagen and periostin expression by cranial neural crest cells during soft palate development. J Histochem Cytochem 2012;60(1):57–68.

[12] Ohki S, Oka K, Ogata K, Okuhara S, Rikitake M, Toda-Nakamura M, et al. Transforming growth factor-beta and sonic hedgehog signaling in palatal epithelium regulate tenascin-C expression in palatal mesenchyme during soft palate development. Front Physiol 2020;11:532.

[13] Itaya S, Oka K, Ogata K, Tamura S, Kira-Tatsuoka M, Fujiwara N, et al. Hertwig's epithelial root sheath cells contribute to formation of periodontal ligament through epithelial-mesenchymal transition by TGF-β. Biomed Res 2017;38(1):61–9.

[14] Ishii M, Arias AC, Liu L, Chen YB, Bronner ME, Maxson RE. A stable cranial neural crest cell line from mouse. Stem Cells Dev 2012;21:3069–80.

[15] Yoshimoto S, Taguchi M, Sumi S, Oka K, Okamura K. Establishment of a novel protocol for formalin-fixed paraffin-embedded organoids and spheroids. Biol Open 2023;12(5):bio059882.

[16] Yamamoto M, Kawashima N, Takashino N, Koizumi Y, Takimoto K, Suzuki N, et al. Three-dimensional spheroid culture promotes odonto/osteoblastic differentiation of dental pulp cells. Arch Oral Biol 2014;59(3):310–7.

[17] Chiquet-Ehrismann R, Chiquet M. Tenascins: regulation and putative functions during pathological stress. J Pathol 2003;200(4):488–99.

[18] Midwood SK, Chiquet M, Tucker PR, Orend G. Tenascin-C at a glance. J Cell Sci 2016;129(23):4321–7.

[19] Chiquet-Ehrismann R, Tucker RP. Tenascins and the importance of adhesion modulation. Cold Spring Harb Perspect Biol 2011;3(5):a004960.

[20] Gang L, Oka K, Ohki S, Rikitake M, Itaya S, Tamura S, et al. CO2 laser therapy accelerates the healing of ulcers in the oral mucosa by inducing the expressions of heat shock protein-70 and tenascin C. Histol Histopathol 2019;34(2):175–89.

[21] Thesleff I, Mackie E, Vainio S, Chiquet-Ehrismann R. Changes in the distribution of tenascin during tooth development. Development 1987;101(2):289–96.

[22] Piva E, Tarquínio SBC, Demarco FF, Silva AF, Araújo VCD. Immunohistochemical expression of fibronectin and tenascin after direct pulp capping with calcium hydroxide. Oral Surg Oral Med Oral Pathol Oral Radiol Endod 2006;102(4):e66–71.

[23] Zarrabi MH, Javidi M, Jafarian AH, Javidi M, Joushan B. Immunohistochemical expression of fibronectin and tenascin in human tooth

pulp capped with mineral trioxide aggregate and a novel endodontic cement. J Endod 2011;37(12):1613–8.

[24] Baldissera EZ, Silva AFD, Gomes APN, Etges A, Botero T, Demarco FF, et al. Tenascin and fibronectin expression after pulp capping with different hemostatic agents: a preliminary study. Braz Dent J 2013;24(3):188–93.

[25] Ye L, MacDougall M, Zhang S, Xie Y, Zhang J, Li Z, Lu Y, Mishina Y, Feng JQ. Deletion of dentin matrix protein-1 leads to a partial failure of maturation ofpredentin into dentin, hypomineralization, and expanded cavities of pulp and root canal during postnatal tooth development. J Biol Chem 2004;279(18):19141–8.

[26] Qin C, D'Souza R, Feng JQ. Dentin matrix protein 1 (DMP1): new and important roles for biomineralization and phosphate homeostasis. J Dent Res 2007;86(12):1134–41.

[27] Zhang M, Zhang X, Luo J, Yan R, Niibe K, Egusa H, et al. Investigate the odontogenic differentiation and dentin-pulp tissue regeneration potential of neural crest cells. Front Bioeng Biotechnol 2020;8:475.

FIGURE LEGENDS

Figure 1. Schematic of the KENZAN method

A, B) O9-1 cells were cultured in 2D plates and transferred to non-adhesion plates. C) The O9-1 spheroids were formed using the bio-ink of the bio-3D printer. D) The spheroids were pierced by microneedles using the bio-3D printer. E) Spheroids were cultured on the microneedles of the kenzan so that they fused with each other. F) The scaffold-free cell construct was retrieved from the kenzan.

Figure 2. Size variation and histological analysis of spheroids created using O9-1 cells

A, B) Variations in O9-1 spheroid size with cell densities of 1.0–5.0 $\times 10^4$ cells/well. Cells were cultured in ES cell medium or EGM/FGM. The graphical displays show spheroid diameter assessed from Day 1 to Day 3. Error bars represent the standard error (n = 16). **C, D)** HE staining and Ki-67 immunohistochemical staining of O9-1 spheroids cultured with ES cell medium. Ki-67-positive cells are observed in the outer layer and central region. **E, F)** HE and Ki-67 immunohistochemical staining of O9-1 spheroids cultured with EGM/FGM. Ki-67-positive cells are found in the central region. Cell nuclei are

stained with hematoxylin. **G, H)** Ki-67-positivity rate of the inner and outer layers of spheroids cultured in ES cell medium and EGM/FGM. Data are presented as box plots showing the median, interquartile range, and full range (n = 4). Scale bars = 100 μm.

* P <0.05.

Figure 3. Comparison of expressions of tenascin C and periostin between 2D and spheroid cultures

A–C) mRNA expressions of type I collagen, periostin and tenascin C in O9-1 cells from 2D culture and O9-1 spheroids. **D, E)** Immunohistochemical staining for periostin and tenascin C in O9-1 spheroids cultured with ES cell medium. Cell nuclei are stained with hematoxylin. **F, G)** Immunohistochemical staining of periostin and tenascin C in O9-1 spheroids cultured with EGM/FGM. Cell nuclei are stained with hematoxylin. Scale bars = 100 μm. The mRNA expression level of each gene is normalized to that of glyceraldehyde 3-phosphate dehydrogenase (Gapdh). Data are presented as box plots showing the median, interquartile range and full range (n = 4). * P<0.05, vs. 2D culture (Mann–

Whitney U test). The black arrowhead indicates the tenascin C expression area. The white (blank) arrowhead indicates the non-tenascin C expression area.

Figure 4. Comparison of the expression of Ki-67, tenascin C, and DMP1 in 2D and spheroid cultures

A–E) Real-time PCR analysis of mRNA expressions for Runx2, Osterix, ALP, DSPP, and DMP1 in cultured O9-1 cells in 2D culture and spheroids. **F)** HE staining of O9-1 spheroids cultured in ES medium. **G–J)** Expressions of Ki-67, and tenascin C (immunohistochemistry), DSPP, and DMP1 (in situ hybridization) in O9-1 spheroids cultured in ES medium. **K–O)** Enlarged views of the dotted squares in F, G, H, I, and J, respectively. Cell nuclei are stained with hematoxylin. Scale bars = 100 μm.

Figure 5. Trial of creating 3D constructs with O9-1 spheroids using the KENZAN-type bio-3D printer

A) Schedule for creating 3D constructs. Day 0: 4.0×10^4 O9-1 cells were seeded in an uncoated plate. Day 3: Spheroids had formed. Day 5: Printing. Day 12: 3D construct formed. **B)** After forming spheroids on day 3. **C)** Each spheroid was

loaded onto microneedles (Day 5) in the KENZAN-type bio-3D printer. **D)** Each spheroid was connected using microneedles (Day 8). **E)** The 3D construct as a single mass after each spheroid was completely connected (Day 12).

Figure 6. Histological analysis of the 3D construct of O9-1 cells cultured with ES cell medium

A) HE staining of the O9-1 3D construct cultured with ES cell medium. **B–E)** Expressions of Ki-67, and tenascin C (immunohistochemistry), DSPP, and DMP1 (in situ hybridization) in the 3D construct cultured with ES cell medium. Scale bars = 300 μm. **F–J)** Enlarged views of the dotted squares in A, B, C, D, and E, respectively. Scale bars = 150 μm.

Figure 7. Histological analysis of the 3D construct of O9-1 cells cultured with calcification induction medium

A) HE staining of the O9-1 3D construct cultured with calcification induction medium. **B–E)** Expressions of Expressions of Ki-67, and tenascin C (immunohistochemistry), DSPP, and DMP1 (in situ hybridization) in the O9-1 3D construct cultured using calcification induction medium. Scale bars = 300 μm.

F–J) Enlarged views of the dotted squares in A, B, C, D, and E. Scale bars = 150 μm. K-M) Real-time PCR analysis of mRNA expression of tenascin C, DSPP, and DMP1 in 3D constructs with ES cell medium and calcification induction medium. The mRNA expression level of each gene was normalized to that of glyceraldehyde 3-phosphate dehydrogenase (Gapdh). Data are presented as box plots showing the median, interquartile range, and full range (n = 4). * P <0.05.

Table 1. Primers used for real-time polymerase chain reaction

Gene	Primer sequences	
	Forward	Reverse
Glyceraldehyde 3-phosphate dehydrogenase(Gapdh)	5'-TGTGTCCGTCGTGGATCTGA-3'	5'-TTGCTGTTGAAGTCGCAGGAG-3'
Type I collagen(Col1)	5'-GGGTCCCTCGACTCCTACA-3'	5'-TGTGTGCGATGACGTGCAAT-3'
Periostin(Postn)	5'-CAGTTGGAAATGATCAGCTCTTGG-3'	5'-CAATTTGGATCTTCGTCATTGCAG-3'
Tenascin C (TnC)	5'-GGAGCAAGCTGATCCAAACCA-3'	5'-CCAGTGCTTGAGTCTTGTCACCA-3'
Runt-related transcription factor-2(Runx2)	5'-GCCCAGGCGTATTTCAGA-3'	5'-TGCCTGGCTCTTCTTACTGAG-3'
Osterix(Osx)	5'-GAAAGGAGGCACAAAGAAG-3'	5'-CACCAAGGAGTAGGTGTGTT-3'
Alkaline phosohatase(ALP)	5'-ATCTTTGGTCTGGCTCCCATG-3'	5'-TTTCCCGTTCACCGTCCAC-3'
Dentin sialophosphoprotein (Dspp)	5'-GGAACTGCAGCACAGAATGA-3'	5'-CAGTGTTCCCCTGTTCGTTT-3'
Dentin matrix protein 1 (Dmp1)	5'-CATCCCAATATGAAGACTG-3'	5'-ACTTTCTTCTGATGACTCA-3'

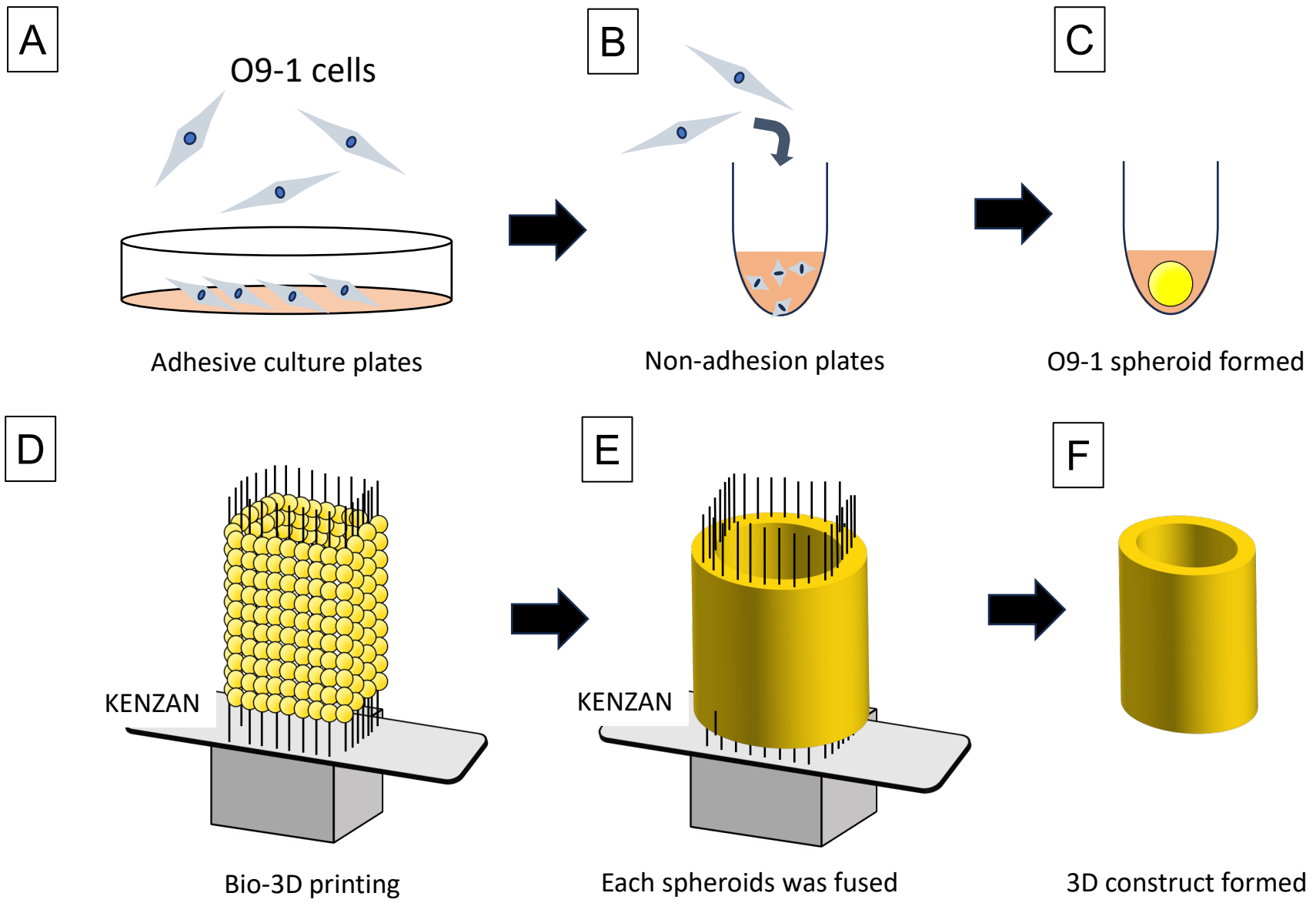

Figure 1. Taguchi et al.,

A

Es Cell medium

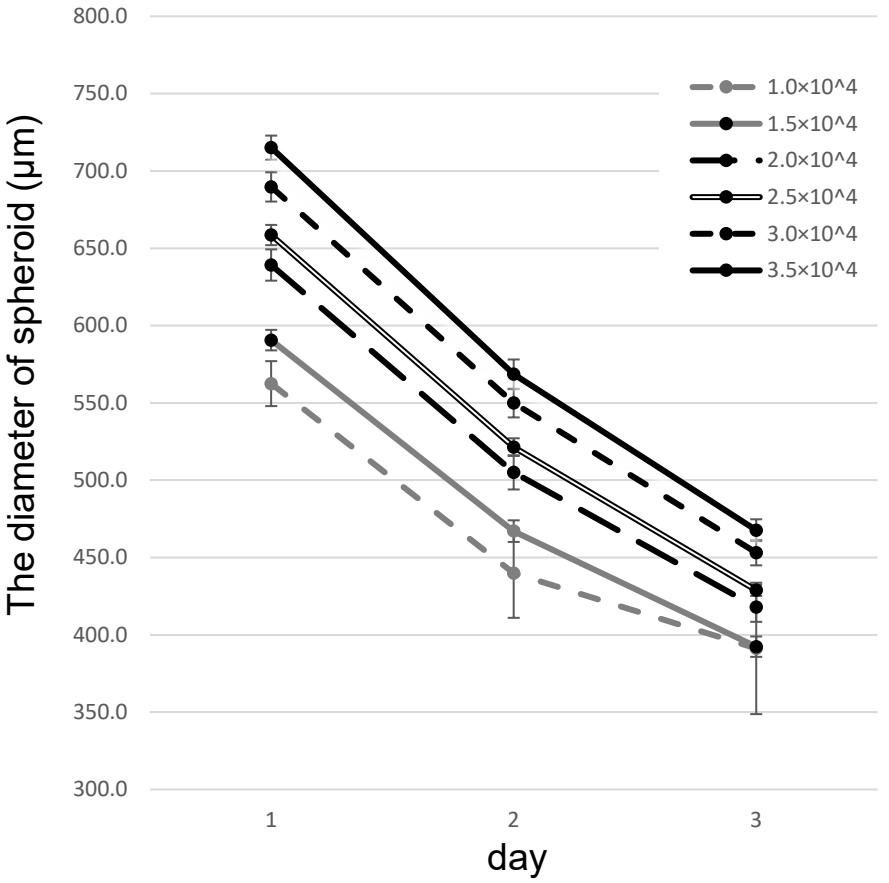

B

EGM/FGM

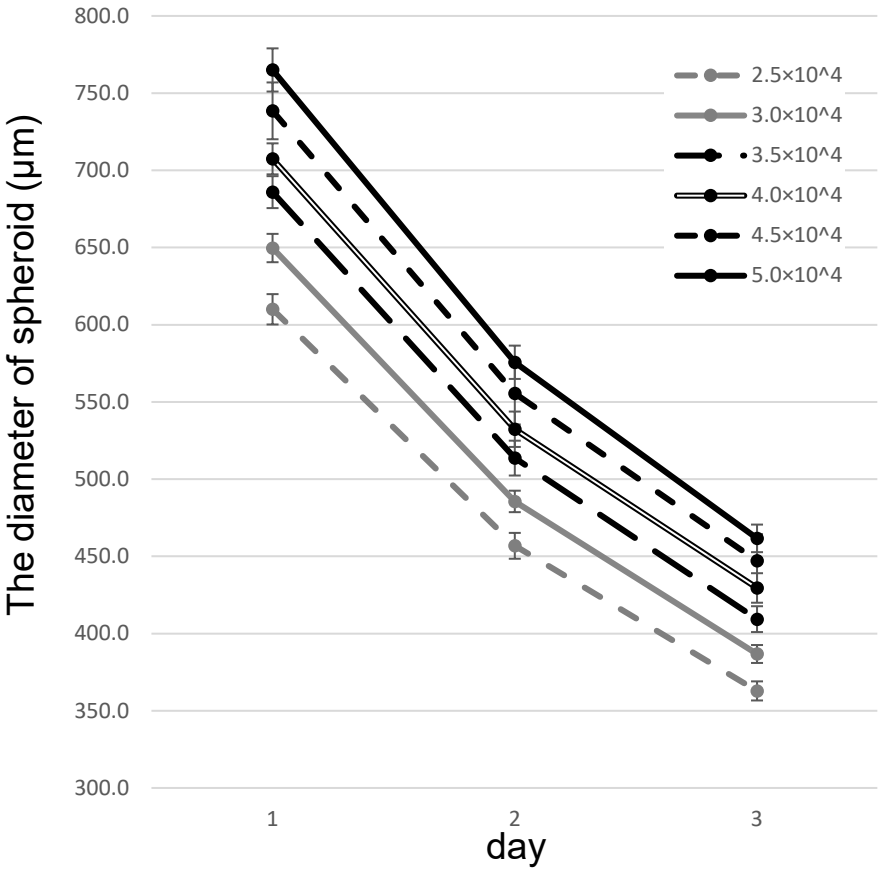

C

HE

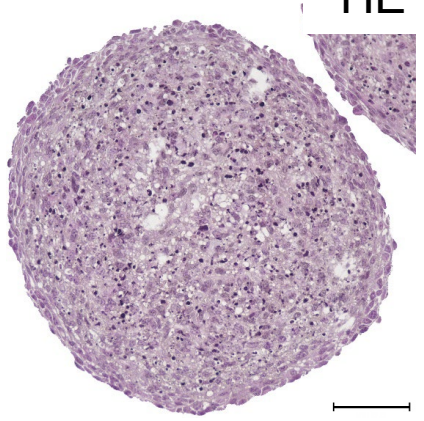

D

Ki-67

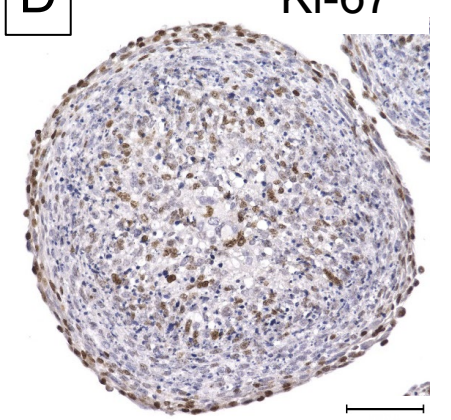

E

HE

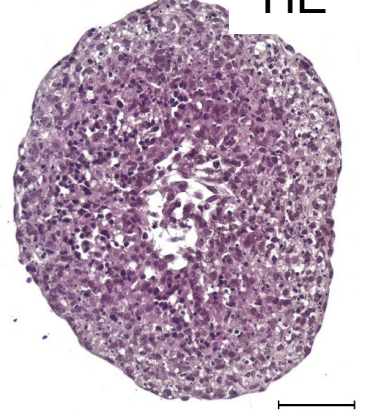

F

Ki-67

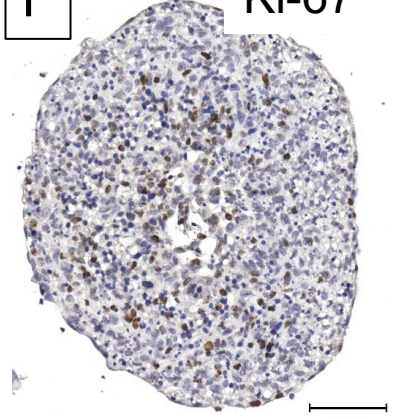

G

ES Cell Medium

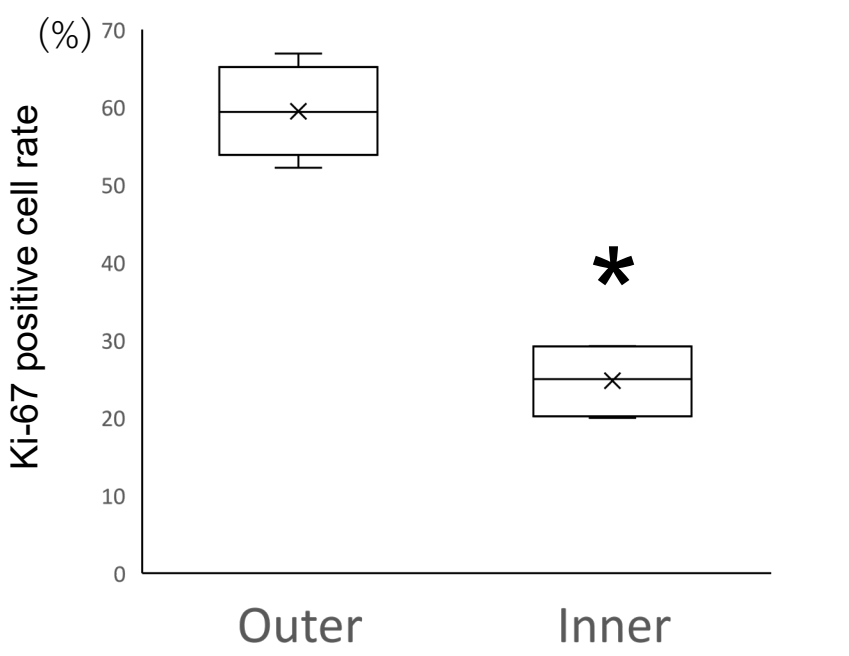

H

EGM/FGM

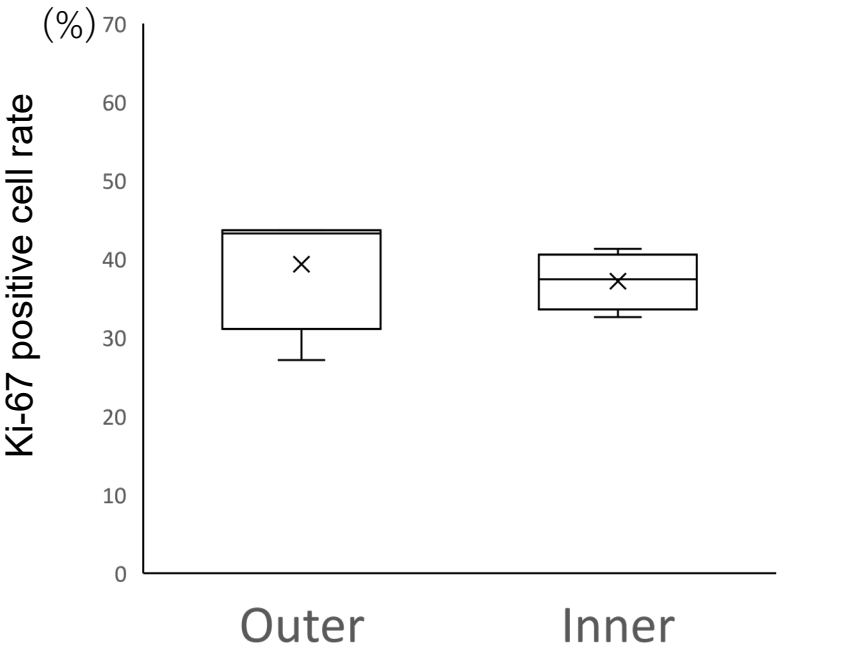

Figure 2. Taguchi et al.,

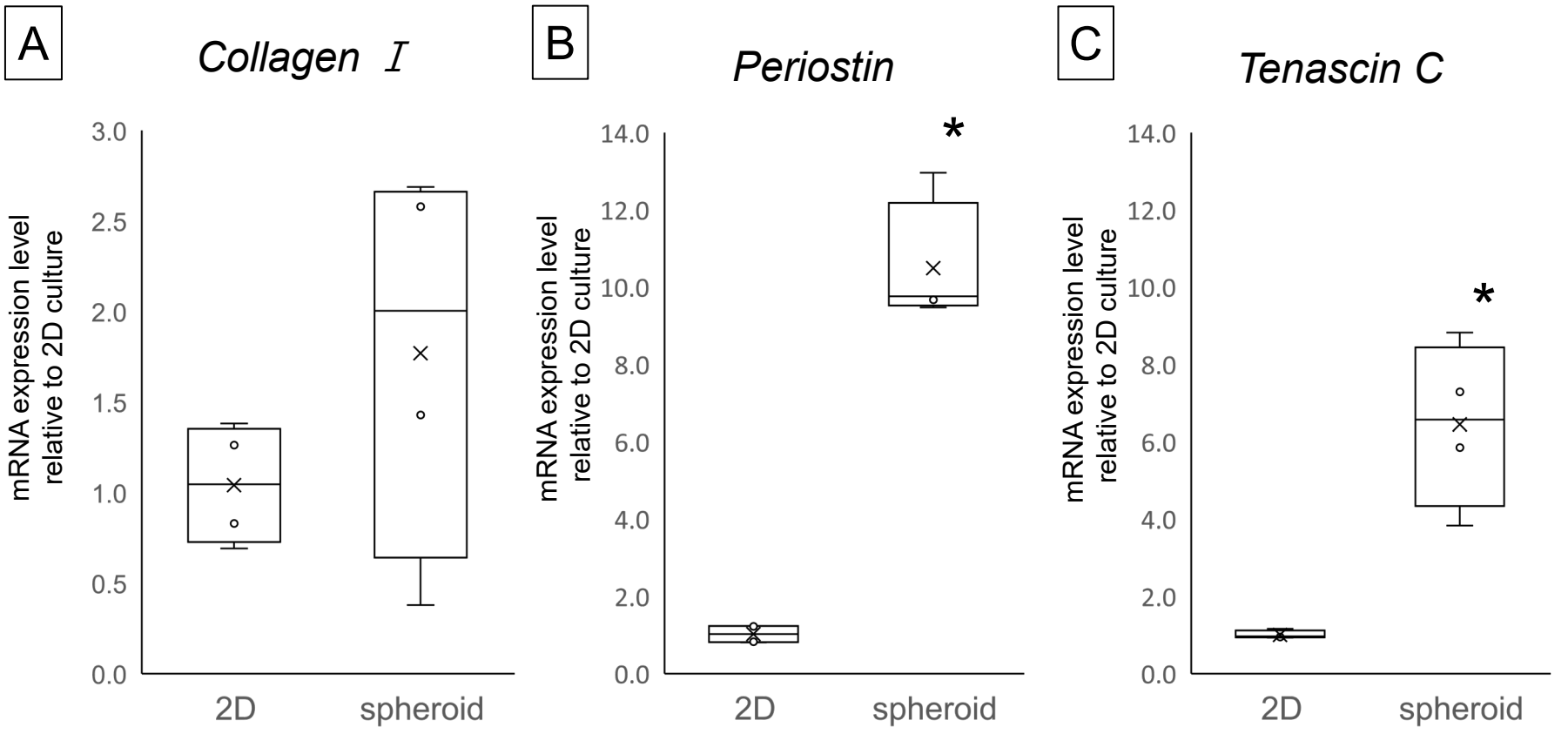

Figure 3. Taguchi et al.,

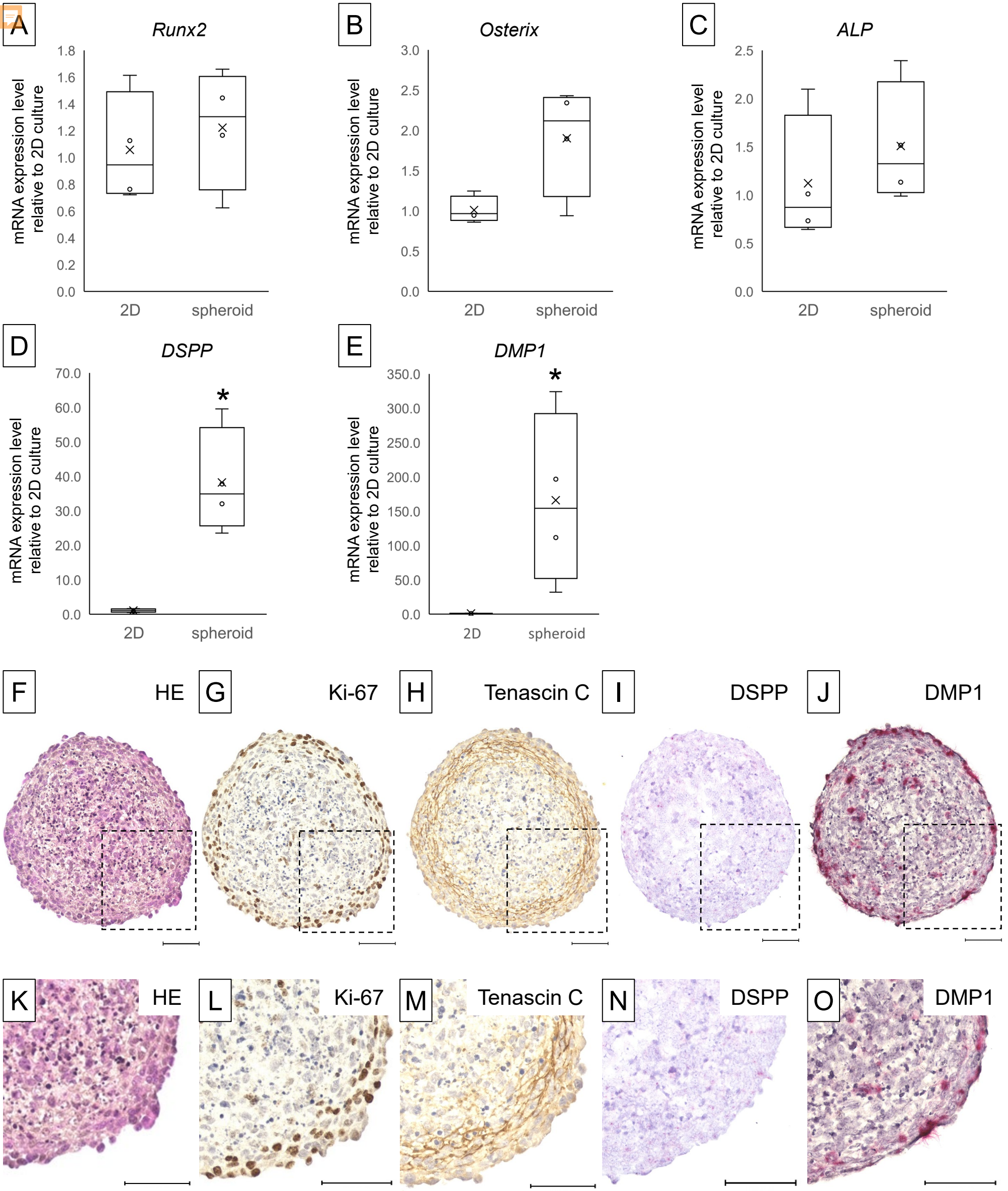

Figure 4. Taguchi et al.,

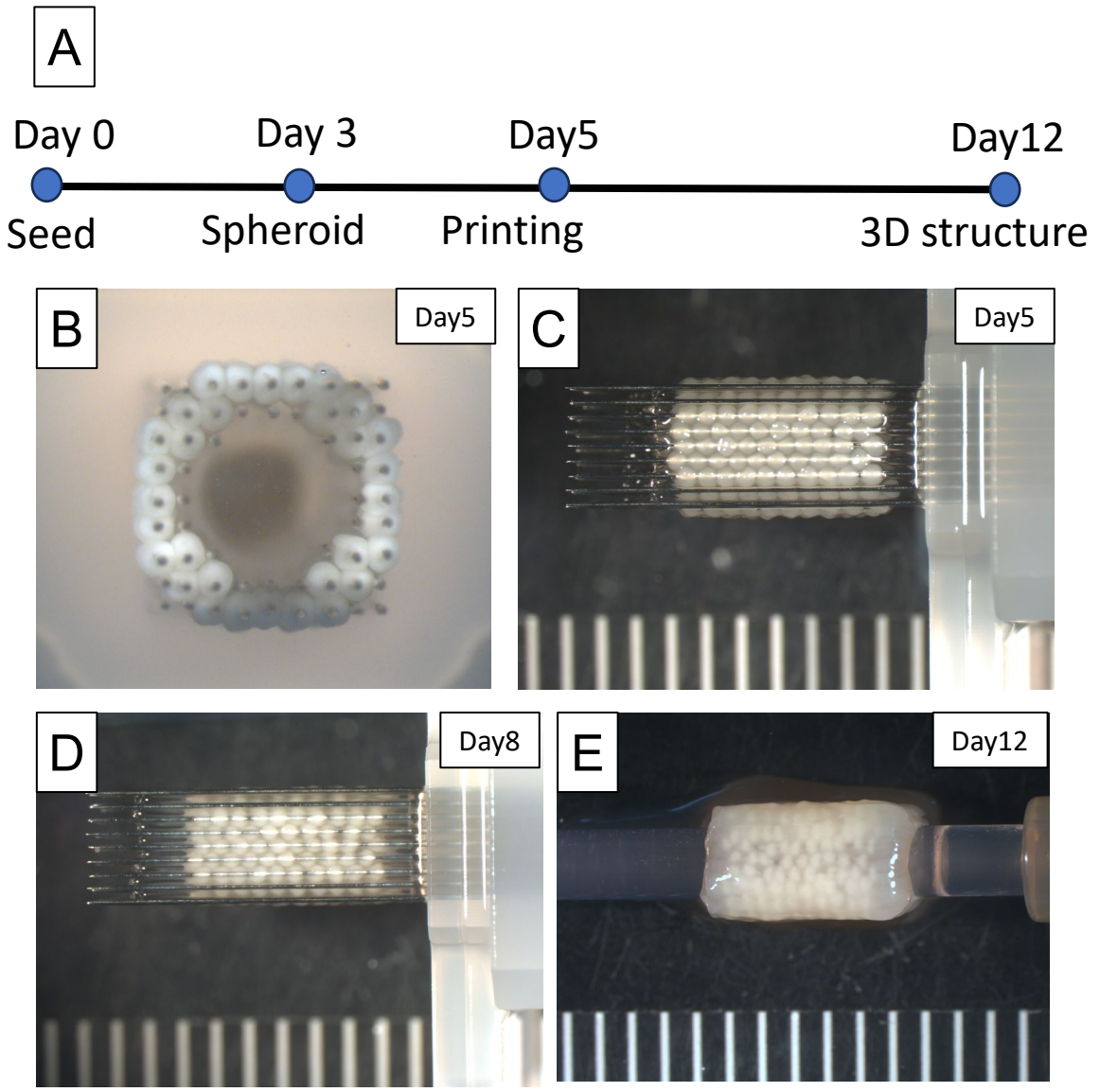

Figure 5. Taguchi et al.,

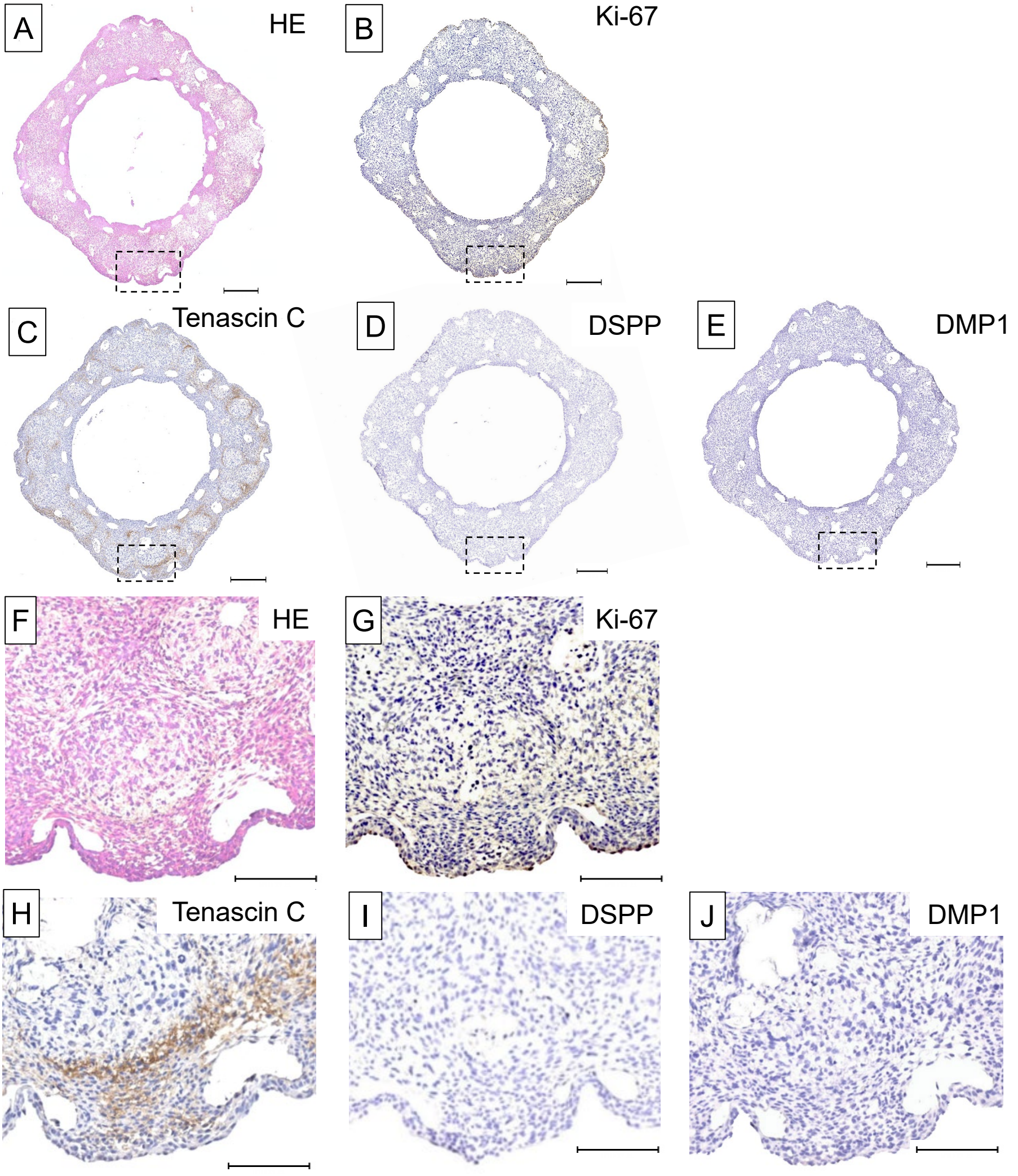

Figure 6. Taguchi et al.,

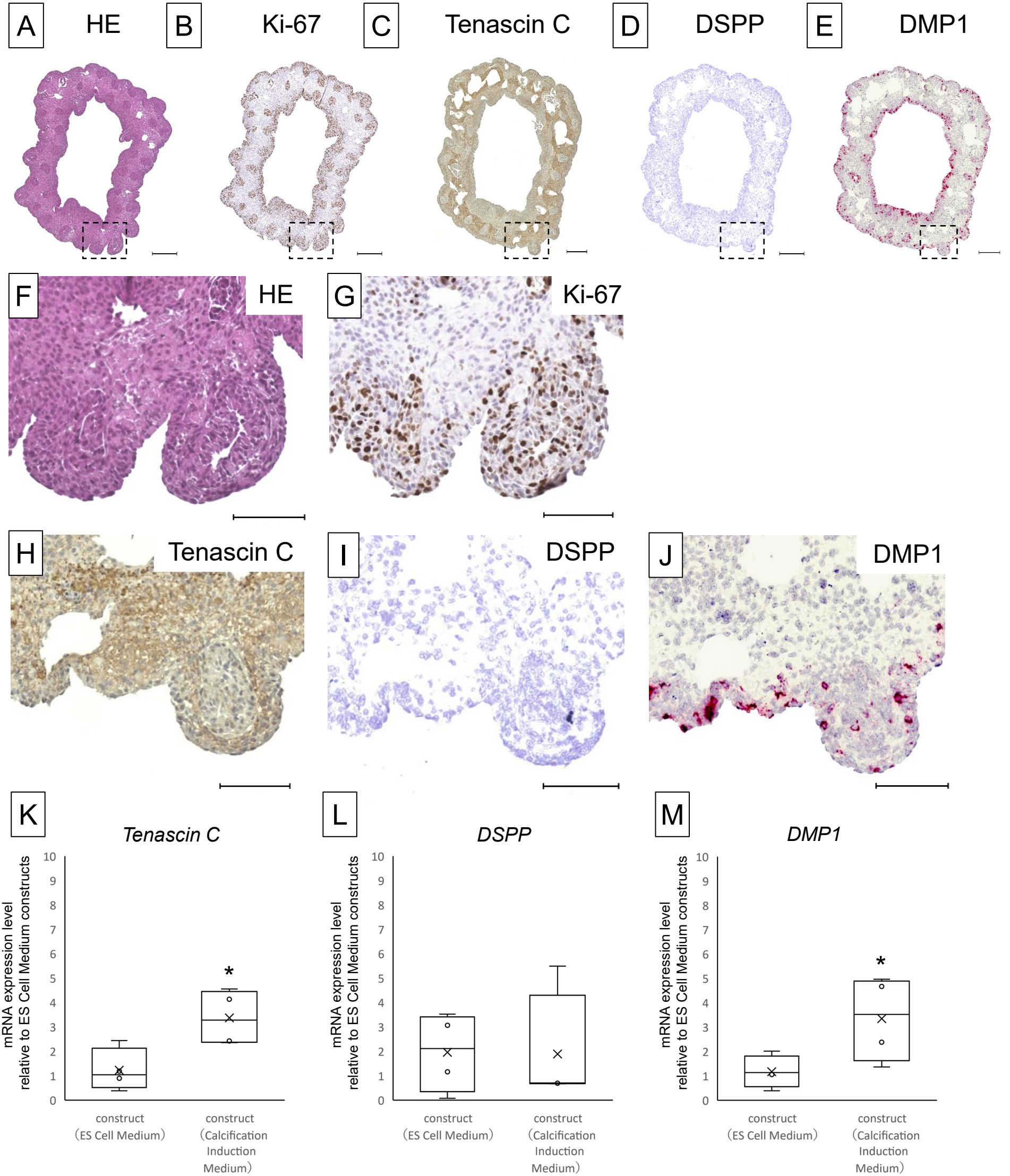

Figure 7. Taguchi et al.,